To the editor:

Metabolic reprogramming of bone marrow stromal cells by leukemic extracellular vesicles in acute lymphoblastic leukemia

Suzanne M. Johnson,[1] Clare Dempsey,[1] Amy Chadwick,[2] Stephanie Harrison,[1] Jizhong Liu,[1] Yujun Di,[1] Owen J. McGinn,[1] Marco Fiorillo,[2] Federica Sotgia,[2] Michael P. Lisanti,[2] Mayur Parihar,[3] Shekhar Krishnan,[4] and Vaskar Saha[1,4]

[1]Children's Cancer Group, and [2]Manchester Centre for Cellular Metabolism, Institute of Cancer Sciences, Manchester Academic Health Sciences Centre, University of Manchester, Manchester, United Kingdom; [3]Tata Medical Center, Kolkata, India; and [4]Tata Translational Cancer Research Centre, Kolkata, India

Cancer cells produce unique heterogeneous vesicles[1] capable of transferring oncogenic material[2,3] to other cells,[4,5] with the potential of modulating a tumor-supportive environment.[6-8] We have previously reported the presence of lipid-enriched, membrane-bound subcellular vesicles at the periphery of acute lymphoblastic leukemia (ALL) cell lines.[9,10] We now extend these findings to describe heterogeneous anucleate vesicles released into extracellular fluids in vitro and in vivo by primary B-cell precursor (BCP) ALL blasts and cell lines. Leukemic extracellular vesicles (LEVs) were internalized by stromal cells, and induced a metabolic switch.

Extracellular vesicles (EVs) are enclosed in lipid bilayers originating from the cell of origin, released by both normal and cancer cells.[1] Here, the BCP cell-specific membrane protein CD19 present within membrane lipid rafts[11] was used to identify the cell of origin of EVs in clinical samples. We directly compared plasma samples from $CD19^+$ primary BCP-ALL bone marrow aspirates at diagnosis containing >95% malignant blasts with matched remission samples obtained after 28 days of therapy (Figure 1A, left panel). The diagnostic sample, which predominantly contained BCP-ALL cells, was significantly enriched in $CD19^+$ vesicles, suggesting that the $CD19^+$ LEVs identified were of leukemic origin. By contrast, $CD61^+$ EVs were increased in remission marrow samples as expected in a regenerating marrow (Figure 1A, right panel). NOD.Cg-*Prkdc*^{scid} *Il2rg*^{tm1Wjl}/SzJ (NSG) mice are extensively used as a patient-derived xenograft model of BCP-ALL, by us[10,12] and others. PKH26-labeled[13] BCP cell line SD1 and LEVs derived from SD1 cells were separately transplanted intrafemorally into NSG mice. Bone marrow flushes taken 17 days later showed transplanted LEVs within a proportion of murine bone marrow stromal cells (BMSCs) (Figure 1B, upper). When labeled SD1 cells were introduced (Figure 1B, lower), cells and LEVs were detected within the extracellular space. Confocal microscopy and 3-dimensional modeling confirmed LEV internalization of prelabeled SD1 LEVs by BMSCs after 24 hours in vitro coincubation (Figure 1C). All transplanted mice showed evidence of $PKH26^+$, human $CD19^+$, or dual$^+$ LEVs in peripheral blood plasma (Figure 1D), and femoral flushes (day 14) showed engrafted $PKH26^+$ ALL cells and murine stromal cells with internalized $PKH26^+$ LEVs (Figure 1E).

The effect of LEV internalization by BMSCs was investigated in the human mesenchymal stem cell line HS5[14] exposed to LEVs released by the BCP-ALL cell lines SD1 and NALM6. Proliferation and viability assays revealed no significant differences from control (Figure 2A). Despite a sustained increase in AKT phosphorylation over 24 hours (Figure 2B), nonsignificant reductions in adenosine triphosphate (ATP) concentrations were observed (Figure 2C). Next, the 2 major energy-producing pathways of the cell and parameters of metabolism were assessed. At 24 hours, HS5 + LEVs showed a reduced oxygen consumption rate (OCR) compared with control, were less sensitive to the inhibition of ATP by oligomycin, and did not change OCR when electron transport from ATP generation in the mitochondria was uncoupled (Figure 2D). Disrupting the electron transport chain (rotenone/antimycin A) reduced OCR to a comparable level in all cells, suggesting that the rate of oxygen consumption from non-mitochondrial sources was comparable. HS5 + LEV have a significantly reduced spare respiratory capacity, an indicator of a decreased ability to respond to stress or metabolic challenge (Figure 2D). Overall, these results suggest that uptake of LEVs significantly reduced mitochondrial respiration in recipient stromal cells.

In the absence of glucose, HS5 and HS5 + LEVs had comparable extracellular acidification rates (ECARs) (Figure 2E). In the presence of glucose, HS5 + LEVs initiated a sharp increase in ECAR compared with control (~fivefold), suggesting a higher glycolytic rate. Inhibiting ATP synthase increased ECAR in both HS5 + LEVs and controls, but more sharply in the latter. Following the addition of 2-deoxy-D-glucose, a competitive inhibitor of glycolysis, ECARs returned to base levels in both control and LEV-exposed cells. Thus, in the presence of glucose, LEV-exposed HS5 showed an increase in ECAR, which is suggestive of glycolysis. This was corroborated by the demonstration of significantly increased extracellular lactate production, the end product of aerobic glycolysis, by HS5 + LEV (Figure 2F). To investigate this further, OCR and ECARs were evaluated in the same cultures simultaneously. A shift toward a glycolytic phenotype was observed in HS5 cells treated with either NALM6 or SD1 LEVs (Figure 2G). Overall, these results suggest that uptake of LEVs significantly reduced mitochondrial respiration in recipient stromal cells and their ability to respond oxidatively to stress or metabolic challenge. Because ATP levels and proliferation rates were similar in HS5 and HS5 + LEV, LEVs induced a metabolic switch from oxidative phosphorylation to aerobic glycolysis in stromal cells to meet energy requirements.

Our observations show that both in vitro and in vivo, BCP-ALL cells release a variety of LEVs into the extracellular fluid and circula-tion that are taken up by BMSCs. LEV-exposed BMSCs undergo a metabolic switch. A similar reprogramming of stromal cells to glycolytic cancer-associated fibroblasts[15,16] has been attributed to exosomes released by chronic lymphocytic leukemia cells.[4] The altered tumor microenvironment promotes leukemic cell survival[17,18] and protects against cytotoxic effects of chemotherapy. A mechanism of this protective effect of the microenvironment appears to be mediated via an adaptation to oxidative stress with decreased mitochondrial electron transfer[12] and a switch to glycolysis.[19] In this study, we show that the reprogrammed stromal cells generate an excess of lactate, which is released into the extracellular fluid. We speculate that this lactate is used preferentially by tumor cells as a source of energy, a process we have previously termed the reverse Warburg effect.[20] Targeting glycolysis[21] as well as the redox adaptation[12] has been shown to overcome drug resistance in ALL. Modulating the tumor-stromal metabolic interactions offers the development of novel therapeutic strategies to enhance the therapeutic response in ALL and other cancers.

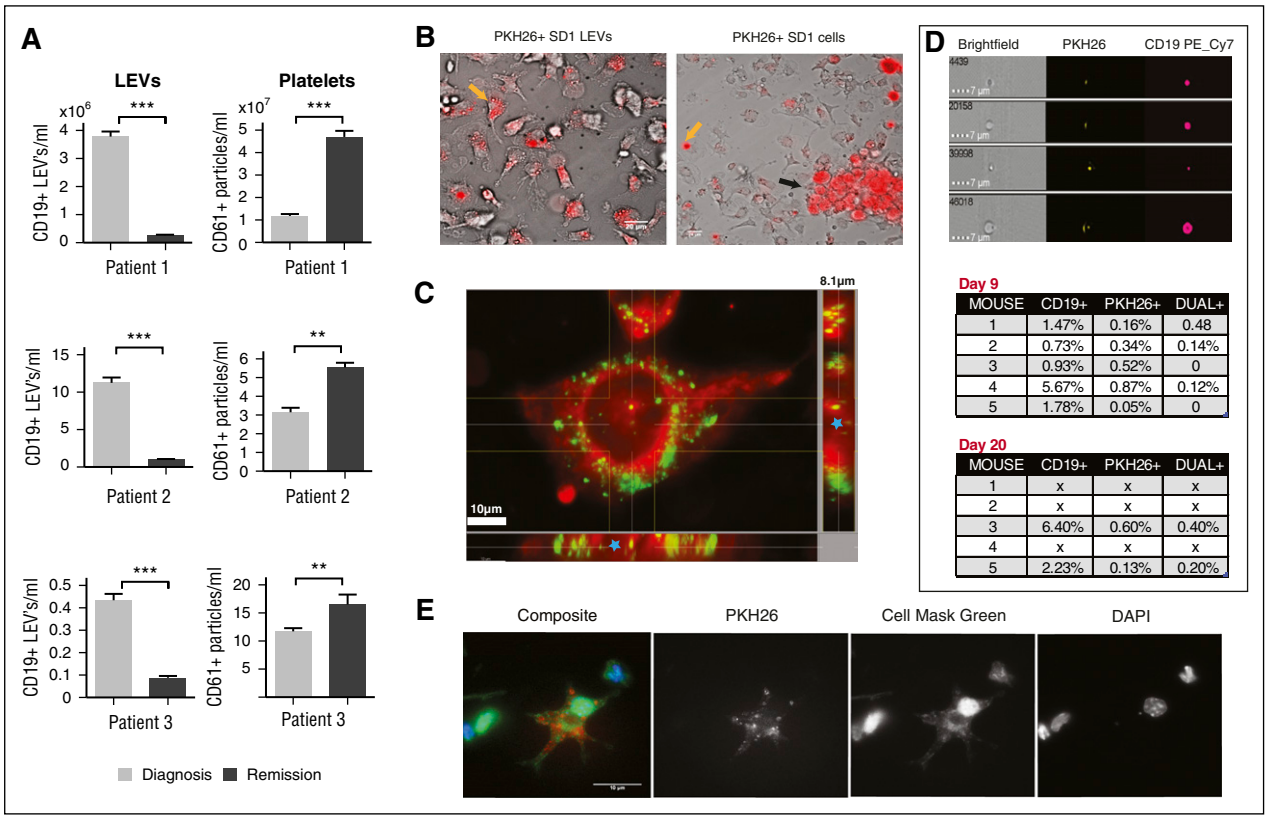

Figure 1. LEVs are produced in vivo and internalized by stromal cells. (A) Diagnostic bone marrow plasma is enriched with $CD19^+$ LEVs. Imaging flow cytometry identified CD19 PE_Cy7 (LEV) and CD61 FITC (platelets)-positive vesicles in matched diagnostic and remission (day 28 postchemotherapy) ALL patient bone marrow plasma samples (1×10^6 events acquired). The number of $CD19^+$ vesicles/mL (LEVs, left) were significantly higher at diagnosis and number of $CD61^+$ extracellular vesicles (platelets, right) significantly higher in remission marrow plasma (**$P > .05$; ***$P > .005$). (B) SD1 cells produce LEVs within the bone marrow microenvironment that are internalized by mouse BMSCs. LEVs from 1×10^7 SD1 cells or 1×10^6 SD1 cells labeled with the fluorescent membrane label PKH26 were introduced into the left femur of 5 NSG mice. Bone marrow flushes taken 17 days posttransplantation were seeded onto fibronectin-coated glass coverslips and BMSCs were allowed to adhere overnight. Live cell images were taken using bright field and ultraviolet illumination with Red Sedat filter at ×40 magnification. Scale bar is 20 µm. The left image represents an overlay of the images and shows murine BMSCs with internalized $PKH26^+$ LEVs as indicated by intracellular red fluorescence (yellow arrow). The figure shows variable, punctate perinuclear red fluorescence within the outer membrane of murine BMSCs and not around the periphery of the recipient cell. The right image shows a cluster of $PKH26^+$ SD1 cells (black arrow) and free $PKH26^+$ LEVs (yellow arrow) in the extracellular space, produced within the murine bone marrow. Scale bar is 20 µm. (C) Confirmation of LEV internalization by human bone marrow cells in vitro. Isolated SD1 LEVs were labeled using a lipophilic tracer (Dio C_{18}; green). Labeled LEVs were added to cultures of bone marrow cells in glass plates for 24 hours. Cells were fixed using paraformaldehyde and counterstained using Cell Mask (red). Serial images were captured at 0.1-µm intervals in Z using a Spinning disk confocal system based around an Olympus IX71 microscope. Illumination achieved by white light LED and a 300-W Xenon light source for fluorescence and Sedat filters. Composite 3-dimensional image from 81 0.1-µm Z stacks was achieved using IMARIS software (BITPLANE, Oxford Instruments) which revealed the LEVs to be fully internalized by the recipient cells as represented by green fluorescence along the midline (indicated by a blue star). Scale bar represents 10 µm. (D) Human $CD19^+$ LEVs are detected in peripheral blood plasma in mice engrafted with primary ALL cells. Plasma samples isolated from tail vein bleeds 9 or 20 days after intrafemoral injection of PKH26-labeled human ALL cells were screened for PKH26 and human $CD19^+$ vesicles. (Top) Synchronus Image stream acquisition of bright field (left), PKH26 (center), and CD19 PE_Cy7 (right) fluorescence-identified vesicles, which originated from the labeled human ALL cells, 9 days posttransplantation. All transplanted mice (n = 5) showed evidence of $PKH26^+$ or human $CD19^+$ vesicles in the peripheral blood plasma. Because $PKH26^+$ LEVs were generated in vivo by transplanted $PKH26^+$ ALL cells, staining is less unform compared with the human $CD19^+$ antibody labeling postisolation. The figure shows dual-labeled LEVs from 10 000 acquired events. Scale bar is 7 µm. (Lower): All transplanted mice showed evidence of $PKH26^+$ or human $CD19^+$ (0.73-5.67% at day 9; 2.23-6.40% at day 20) LEVs in the peripheral blood plasma. (E) Engrafted primary human ALL cells introduced into the mouse bone marrow produce LEVs that are internalized by surrounding mouse BMSCs. Primary ALL cells were labeled with PKH26 (red) and introduced into the femur of 5 NSG mice. Bone marrow flushes 14 days after injection were seeded onto fibronectin and fixed with paraformaldehyde. Cells were counterstained with cell mask green and 4′,6-diamidino-2-phenylindole. The panel shows $PKH26^+$ LEVs, visualized as punctate red fluorescent staining within the cell membrane of adherent mouse BMSCs, were internalized by mouse BMSCs in vivo (×160 magnification). Captured using black and white film, the figure shows composite image and individual filters. Scale bar is 10 µm.

The HS5 cell line was obtained from ATCC and the SD1 and NALM6 from DSMZ.

Animal procedures were approved by Cancer Research UK, Manchester Institute's Animal Welfare and Ethical Review Body, and performed under a project license issued by the United Kingdom Home Office. Six- to 12-week-old NSG mice were transplanted intrafemorally with either 1×10^6 PKH26-labeled ALL cells, SD1 cells, or vesicles from 1×10^7 PKH26-stained ALL cells. Bone marrow flushes from transplanted mice were seeded onto fibronectin and either imaged live or fixed with 3.7% paraformaldehyde and counterstained with Cell Mask green (Life Technologies) and 4′,6-diamidino-2-phenylindole.

To assess BMSC metabolism, HS5 cells were seeded at 1×10^4 cells/well, whereas SD1 or NALM6 were cultured in serum-free RPMI. Dulbecco's modified Eagle medium diluted 1:1 with either serum-free RPMI or LEV-containing conditioned media was added and incubated for 24 hours. HS5 ± LEVs were washed and replated into XF^{e}96 FluxPaks before equilibration in basal media. The response to both glycolytic and mitochondrial stress was analyzed on using a Seahorse XF^{e}96 extracellular flux analyzer (Seahorse Bioscience, Bothell, MA).

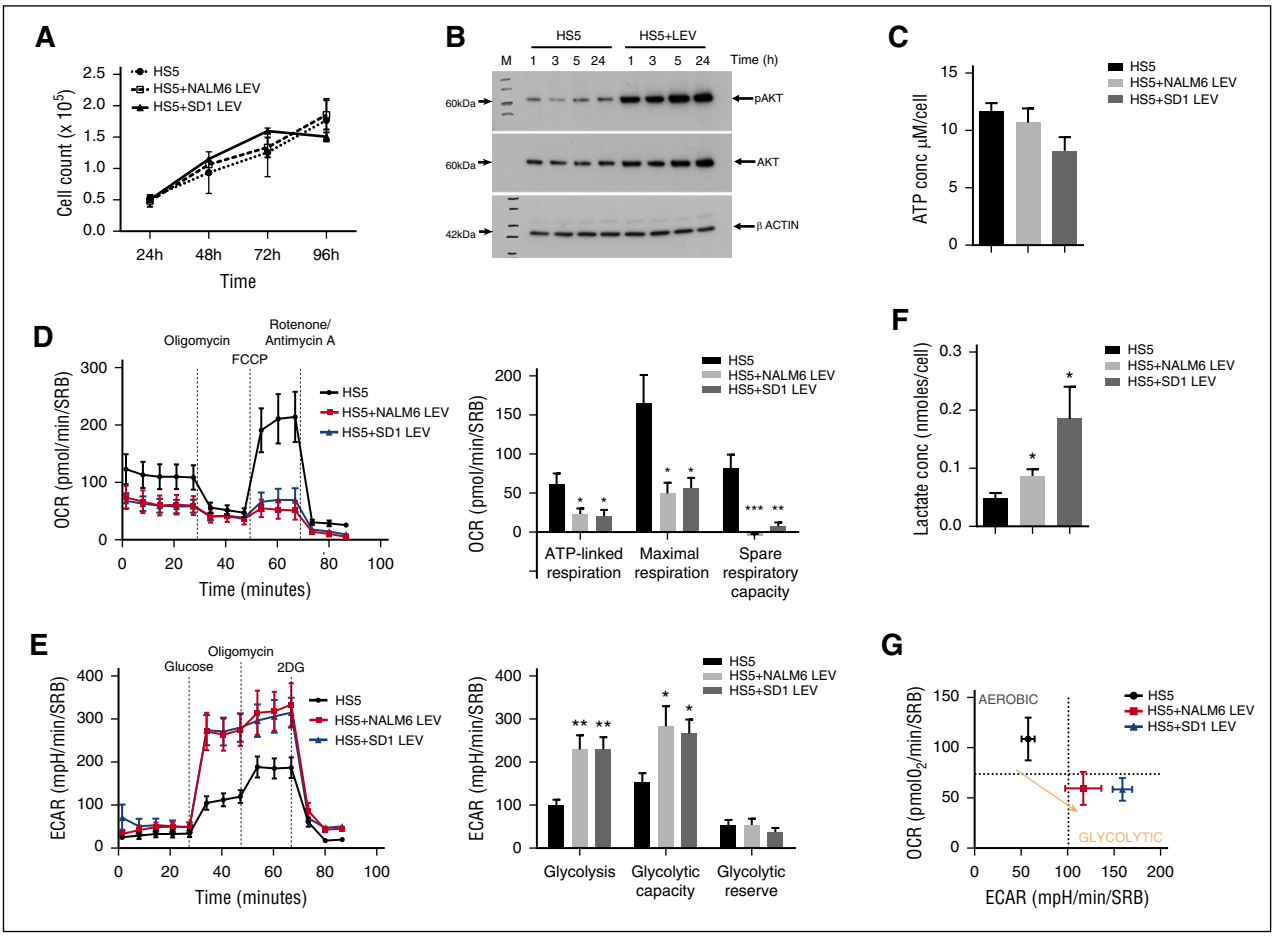

Figure 2. LEV uptake by BMSCs alters cell metabolism. (A) LEV uptake by BMSCs did not affect the survival or proliferation of BMSCs. HS5 cells were plated into 96-well plates at 4×10^4 cells per well. Unselected LEVs were isolated from serum-free cultures of SD1 and NALM6 cells. LEV-containing conditioned media (24 hours) was diluted 1:1 with Dulbecco's modified Eagle medium (DMEM)/10% fetal bovine serum (FBS) and added to the HS5 cells. A 3-(4,5 dimethylthiazol-2-yl)-5-(3-carboxymethoxyphenyl-2-(4-sulfophenyl)-2H-tetrazolium assay was used to assess proliferation and viability of HS5 cells; HS5 + NALM6 LEVs and HS5 + SD1 LEVs over 96 hours. At least 5 wells were assessed at each time point and the experiment repeated 3 times. No significant differences were apparent. (B) Coincubation of BMSCs with ALL LEVs results in activation of AKT. HS5 cells were seeded into large 10-cm cell culture plates at 1.5×10^5 cells and allowed to adhere. LEVs were isolated from 24-hour serum-free RPMI cultures of SD1 cells. HS5 media were replaced with LEV containing conditioned media diluted 1:1 with DMEM/10% FBS and incubated at 37°C 5% CO_2. Cells were washed and lysed on ice at 1, 3, 5, and 24 hours. A 30-μg protein was resolved by gradient sodium dodecyl sulfate-polyacrylamide gel electrophoresis and transferred to polyvinylidene difluoride membrane. Blots were probed for pAKT, and then reprobed for AKT and β-Actin. The figure shows increased pAKT in HS5 + LEV compared with control across all time points and is representative of 3 independent experiments. (C) ATP production by BMSC + LEV is reduced compared with control BMSCs. ATP production was measured using the Cell Titer Glo assay (Promega) in HS5 cells exposed to LEVs from either NALM6 or SD1 cells for 24 hours. Data are mean and standard error of the mean (SEM) of 4 independent experiments. (D) BMSC + LEVs have lower resting energetics and are less able to respond to metabolic challenge. HS5 cells were seeded into Seahorse XFe96 cell plates at 1×10^4 cells per well and allowed to attach. LEV-containing conditioned media were diluted 1:1 with DMEM/10% FBS and added to the HS5 cells for 24 hours. Cells were washed and equilibrated in basal media. An XF cell mitochondrial stress test was performed and OCR monitored following the sequential addition of oligomycin an inhibitor of ATP synthase, FCCP (carbonyl cyanide *p*-trifluoromethoxyphenylhydrazone), which uncouples electron transport from ATP generation in the mitochondria and rotenone/antimycin A, which in turn disrupts the electron transport chain using the XFe96 extracellular flux analyzer. Individual wells were normalized using sulforhodamine B. LEV uptake resulted in a lower basal respiration rate and diminished ability to respond to energetic crisis in the BMSCs. ATP-linked respiration, maximal respiration and spare respiratory capacity (difference in the basal respiratory rate and the maximal respiration) were all significantly diminished in LEV-exposed BMSCs, indicating oxidative stress. Figures are representative of 3 independent experiments with 6 replicates per plate; error bars represent SEM of a representative experiment. ATP-linked respiration: basal respiration minus proton leak reveals ATP production. Maximal respiration occurs when the uncoupler FCCP stimulates the respiratory chain to operate at its maximum speed and mimics a physiological "energetic crisis" and is measured after oligomycin through to before rotenone and antimycin A injection. Spare respiratory capacity refers to the difference between the maximal FCCP-stimulated rate of respiration minus basal respiration and reflects the cells ability to deal with an energetic crisis. (E) BMSC + LEVs use glucose more readily and have a greater glycolytic capacity. HS5 cells, HS5 + NALM6 LEVs, and HS5 + SD1 LEVs were washed and equilibrated in assay media before basal readings. Glycolysis stress test was performed and the ECAR was monitored following the sequential addition of glucose, oligomycin, and 2-deoxy-D-glucose (2DG, a competitive inhibitor of glycolysis using an XFe96 extracellular flux analyzer). Individual wells were normalized using sulforhodamine B. Glycolysis and glycolytic capacity were significantly increased in the LEV-exposed HS5 cells, whereas the glycolytic reserve was comparable to control cells. Figures are representative of 3 independent experiments with 6 replicates per plate; error bars represent SEM of a representative experiment. Glycolysis as indicated by the first measurement of ECAR (attributed to the breakdown of glucose to pyruvate) taken after glucose addition minus the ECAR before glucose addition. Glycolytic capacity refers to increased rate of glycolysis to meet the metabolic demands of the cell following the addition of oligomycin, which blocks mitochondrial ATP synthase minus ECAR before glucose addition. Glycolytic reserve indicates the increase in glycolysis needed to meet cellular energetic requirements without mitochondrial ATP production as calculated by the glycolytic capacity minus glycolysis measurements. (F) BMSC + LEVs produce more lactate compared with control. HS5 cells were seeded as described and the media harvested after 24 hours. The media from BMSC ± LEV from either SD1 cells or NALM6 cells were screened for lactate 24 hours later and compared with control. An increase in lactate was evident from BMSCs + LEVs from either leukemic cell line. Data are expressed as concentration (nmole/cell) as determined from a standard curve and normalized to individual cell counts. Figures are representative of 3 independent experiments with multiple replicates per plate; error bars represent SEM of a representative experiment. (G) LEV-exposed BMSCs switch to a glycolytic phenotype. HS5 cells were exposed to LEVs from either NALM6 or SD1 cells for 24 hours, then washed and equilibrated in mitochondrial stress test media. Extracellular acidification and oxygen consumption were measured in the same well. Although control HS5 cells maintain aerobic respiration, following exposure to LEVs for 24 hours, they switch to a more glycolytic phenotype and become less dependent on mitochondrial respiration. The figure is representative of 3 independent experiments with 6 replicates per plate; error bars represent SEM of a representative experiment. $^*P < .05$; $^{**}P < .01$; $^{***}P < .005$.

Acknowledgments: This research received funding from the European Union's Seventh Framework Programme for research, technological development, and demonstration (Grant agreement no. 278514 – IntReALL); a program grant from Cancer Research UK; and an Leukaemia and Lymphoma Research project grant. V.S. is the recipient of an India Alliance Margdarshi Fellowship.

Contribution: S.M.J., C.D., and V.S. designed the research; S.M.J., C.D., A.C., S.H., and M.F. performed research; J.L., Y.D., and O.J.M. contributed to data interpretation; F.S. and M.P.L. contributed vital new reagents and analytical tools; S.M.J., C.D., M.P., S.K., and V.S. analyzed and interpreted data; and S.M.J. and V.S. wrote the manuscript.

Conflict-of-interest disclosure: The authors declare no competing financial interests.

Correspondence: Vaskar Saha, Children's Cancer Group, Institute of Cancer Sciences, Manchester Academic Health Sciences Centre, Paterson Building, University of Manchester, 550 Wilmslow Rd, Manchester M20 4BX, United Kingdom; e-mail: vaskar.saha@manchester.ac.uk.

References

1. Raposo G, Stoorvogel W. Extracellular vesicles: exosomes, microvesicles, and friends. *J Cell Biol.* 2013;200(4):373-383.
2. Al-Nedawi K, Meehan B, Micallef J, et al. Intercellular transfer of the oncogenic receptor EGFRvIII by microvesicles derived from tumour cells. *Nat Cell Biol.* 2008;10(5):619-624.
3. Skog J, Würdinger T, van Rijn S, et al. Glioblastoma microvesicles transport RNA and proteins that promote tumour growth and provide diagnostic biomarkers. *Nat Cell Biol.* 2008;10(12):1470-1476.
4. Paggetti J, Haderk F, Seiffert M, et al. Exosomes released by chronic lymphocytic leukemia cells induce the transition of stromal cells into cancer-associated fibroblasts. *Blood.* 2015;126(9):1106-1117.
5. Zomer A, Maynard C, Verweij FJ, et al. In Vivo imaging reveals extracellular vesicle-mediated phenocopying of metastatic behavior. *Cell.* 2015;161(5):1046-1057.
6. Costa-Silva B, Aiello NM, Ocean AJ, et al. Pancreatic cancer exosomes initiate pre-metastatic niche formation in the liver. *Nat Cell Biol.* 2015;17(6):816-826.
7. Webber J, Yeung V, Clayton A. Extracellular vesicles as modulators of the cancer microenvironment. *Semin Cell Dev Biol.* 2015;40:27-34.
8. Peinado H, Alečković M, Lavotshkin S, et al. Melanoma exosomes educate bone marrow progenitor cells toward a pro-metastatic phenotype through MET. *Nat Med.* 2012;18(6):883-891.
9. Patel N, Krishnan S, Offman MN, et al. A dyad of lymphoblastic lysosomal cysteine proteases degrades the antileukemic drug L-asparaginase. *J Clin Invest.* 2009;119(7):1964-1973.
10. Holland M, Castro FV, Alexander S, et al. RAC2, AEP, and ICAM1 expression are associated with CNS disease in a mouse model of pre-B childhood acute lymphoblastic leukemia. *Blood.* 2011;118(3):638-649.
11. Deaglio S, Vaisitti T, Billington R, et al. CD38/CD19: a lipid raft-dependent signaling complex in human B cells. *Blood.* 2007;109(12):5390-5398.
12. Liu J, Masurekar A, Johnson S, et al. Stromal cell-mediated mitochondrial redox adaptation regulates drug resistance in childhood acute lymphoblastic leukemia. *Oncotarget.* 2015;6(40):43048-43064.
13. Lanzkron SM, Collector MI, Sharkis SJ. Hematopoietic stem cell tracking in vivo: a comparison of short-term and long-term repopulating cells. *Blood.* 1999; 93(6):1916-1921.
14. Roecklein BA, Torok-Storb B. Functionally distinct human marrow stromal cell lines immortalized by transduction with the human papilloma virus E6/E7 genes. *Blood.* 1995;85(4):997-1005.
15. Zhang W, Trachootham D, Liu J, et al. Stromal control of cystine metabolism promotes cancer cell survival in chronic lymphocytic leukaemia. *Nat Cell Biol.* 2012;14(3):276-286.
16. Fiaschi T, Marini A, Giannoni E, et al. Reciprocal metabolic reprogramming through lactate shuttle coordinately influences tumor-stroma interplay. *Cancer Res.* 2012;72(19):5130-5140.
17. Boutter J, Huang Y, Marovca B, et al. Image-based RNA interference screening reveals an individual dependence of acute lymphoblastic leukemia on stromal cysteine support. *Oncotarget.* 2014;5(22):11501-11512.
18. Kurtova AV, Balakrishnan K, Chen R, et al. Diverse marrow stromal cells protect CLL cells from spontaneous and drug-induced apoptosis: development of a reliable and reproducible system to assess stromal cell adhesion-mediated drug resistance. *Blood.* 2009;114(20):4441-4450.
19. Jitschin R, Braun M, Qorraj M, et al. Stromal cell-mediated glycolytic switch in CLL cells involves Notch-c-Myc signaling. *Blood.* 2015;125(22):3432-3436.
20. Bonuccelli G, Whitaker-Menezes D, Castello-Cros R, et al. The reverse Warburg effect: glycolysis inhibitors prevent the tumor promoting effects of caveolin-1 deficient cancer associated fibroblasts. *Cell Cycle.* 2010;9(10):1960-1971.
21. Hulleman E, Kazemier KM, Holleman A, et al. Inhibition of glycolysis modulates prednisolone resistance in acute lymphoblastic leukemia cells. *Blood.* 2009; 113(9):2014-2021.

DOI 10.1182/blood-2015-12-688051

To the editor:

Cytomegalovirus replication reduces the relapse incidence in patients with acute myeloid leukemia

Ahmet H. Elmaagacli[1,*] and Michael Koldehoff[2,*]

[1]Department of Hematology/Oncology and Stem Cell Transplantation, Helios Klinik Schwerin, Schwerin, Germany; and [2]Bone Marrow Transplantation, West German Cancer Center, University Hospital Essen, University of Duisburg-Essen, Essen, Germany

Recently, Teira et al published a study for the Center for International Bone Marrow Transplant Research (CIBMTR) showing no benefit of cytomegalovirus (CMV) reactivation for relapse risk in acute myeloid leukemia (AML) patients after transplant.[1] Unfortunately, in this register study, a uniform definition for CMV reactivation was not given, nor were the methods for evaluation of CMV reactivation described; so each participating center defined CMV reactivation differently with a heterogeneously defined cutoff level using different methods. Furthermore, it was not clear whether and how CMV reactivation was consequently treated with antiviral agents in each center as has been done in all other studies about CMV reactivation. This weakness in the study design seriously questions the reliability of the results of this study.[1] In contrast, we and others have published that CMV reactivation correlates with substantially improved reduction of relapse incidence in patients with AML after transplant.[2-10] The antileukemic effect of CMV reactivation is pronounced in AML and chronic myeloid leukemia (CML), but is detectable to a lesser extent in myelodysplastic syndrome (MDS), acute lymphoblastic leukemia (ALL), non-Hodgkin lymphoma, and pediatric acute leukemia.[3-10] We defined this remarkable phenomenon as a virus-versus-leukemia effect, which is rare in hematology and contrary to the effects of oncovirus causing cancer or hematological malignancies such as hepatitis B and C virus, Epstein-Barr virus, human T-lymphotropic virus, Kaposi sarcoma–associated herpes virus, and human papilloma virus.[11]

CMV infects a variety of cells such as endothelial cells, fibroblasts, retinal epithelial cells, bronchial and alveolar cells, neurons,